Article

Studies of C–S Bond Cleavage Reactions of Re(V) Dithiolates: Synthesis, Reactivity, and Mechanism

Ming Li, Arkady Ellern, and James H. Espenson

J. Am. Chem. Soc., **2005**, 127 (29), 10436-10447• DOI: 10.1021/ja0519334 • Publication Date (Web): 28 June 2005

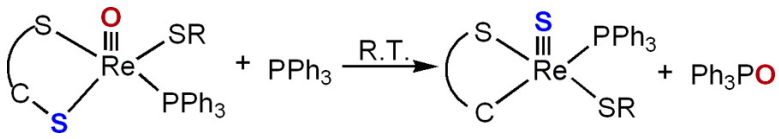

More About This Article

Additional resources and features associated with this article are available within the HTML version:

- Supporting Information
- Links to the 4 articles that cite this article, as of the time of this article download
- Access to high resolution figures
- Links to articles and content related to this article
- Copyright permission to reproduce figures and/or text from this article

View the Full Text HTML

J|A|C|S
ARTICLES
Published on Web 06/28/2005

Studies of C−S Bond Cleavage Reactions of Re(V) Dithiolates: Synthesis, Reactivity, and Mechanism

Ming Li, Arkady Ellern, and James H. Espenson*

Contribution from the Ames Laboratory and Department of Chemistry, Iowa State University, Ames, Iowa 50011

Received March 25, 2005; E-mail: espenson@iastate.edu

Abstract: A series of rhenium(V) complexes, [(X)(ReO)(dt)(PPh_3)] and [(o-$SC_6H_4PPh_2$)(ReO)(mtp)], were prepared to explore electronic effects on the C−S cleavage reaction that occurs upon reaction with PAr_3 at ambient temperature [where X = S(C_6H_4-*p*-Z) (Z = OMe, Me, H, F, Cl), OPh, Cl, and SC_2H_5, and dt is the chelating dithiolate ligand derived from 2-(mercaptomethyl)thiophenol, 1,2-ethanedithiol, 1,3-propanedithiol, 1,3-butanedithiol, and 2,4-pentanedithiol]. The scope and selectivity of the C−S activation were examined. The C−S bond cleavage to form metallacyclic Re(V) complexes with a Re≡S core occurs only for the complexes with mtp and pdt frameworks and X = SAr and SC_2H_5. The difference in reactivity is due to the different donating abilities of ancillary and dithiolate ligands, especially their π-donating ability, which plays a critical role in C−S activation. The kinetics of the C−S activation process was determined; nucleophilic attack of PPh_3 on the oxo group of the $Re^{V}O$ core appears to be the rate-controlling step. The reaction is accelerated by electron-poor ArS ligands, but is unaffected by the substituents on phosphines. A detailed mechanistic study is presented. The results represent a rare example of migration of alkanethiolate leading to the formation of alkylthiolato complexes.

Introduction

The chemical reactivities of oxorhenium(V) complexes containing a chelated dithiolate (dt) ligand[1] pose dramatic contrasts depending on whether the "bystander" ligand is PhS or Me.[2] These chemical equations show the reactions with PPh_3/PAr_3 that occur readily at ambient temperature, illustrating the sharp distinction between the two.

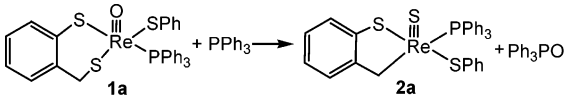

1a 2a (1)

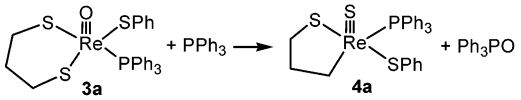

3a 4a (2)

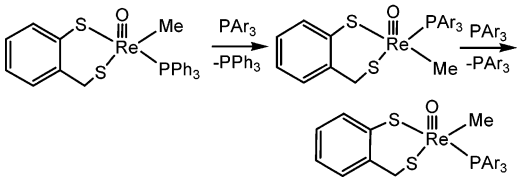

(3)

Equations 1 and 2 represent the results of the evidently complex process that is the principal focus of this article. In the course of these reactions, the Re−O bond is broken, a terminal Re−S bond is made at the expense of C−S−Re bonds, and a C−Re bond is formed. The Me−Re analogue, on the other hand, undergoes only ligand substitution in sequential steps, eq 3.[3]

This article presents new data for the reactions represented by eqs 1 and 2 through variations of the constitution of the rhenium reagents, as shown in the structural formulas for **1**, **3**, **5**, **6**, and **7** in Chart 1. The kinetics of these reactions was studied to determine the chemical mechanism. Additionally, attention has been devoted to understanding the contrasting behavior of the PhS−Re and Me−Re compounds in light of further findings concerning [XReO(dt)(PPh_3)], **5** and **6**, where X = Cl, PhO, and EtS in addition to PhS.

Results

Synthesis of Rhenium(V) Complexes. The most efficient route to monomeric oxorhenium(V) complexes is by reaction of the more readily prepared dimers.[4] In this study, compounds **1** and **5b** were prepared by converting the recently reported,[5] brown-colored dimers, {PhSReO(dt)}$_2$, to the green monomers, [PhSReO(dt)(PPh_3)], by reaction with a *controlled quantity* of PPh_3, namely a 1:2 ratio of dimer to PPh_3. The products were characterized by ^{1}H and ^{31}P NMR spectroscopy and by elemental analysis. The experimental details for these reactions, shown in Scheme 1, are described in the Experimental Section. These reactions proceed in high yield for dt = mtp and edt

(1) Abbreviations: $mtpH_2$, 2-(mercaptomethyl)thiophenol; $edtH_2$, 1,2-ethanedithiol; $pdtH_2$, 1,3-propanedithiol; $pdtMeH_2$, 1,3-butanedithiol; $pdtMe_2H_2$, 2,4-pentanedithiol. Stand-alone formulas for the ligands *in complexes* are written as mtp, edt, etc., without charge being shown.

(2) Li, M.; Ellern, A.; Espenson, J. H. *Angew. Chem., Int. Ed.* **2004**, *43*, 5837−5839.

(3) Lahti, D. W.; Espenson, J. H. *J. Am. Chem. Soc.* **2001**, *123*, 6014−6024.

(4) Jacob, J.; Lente, G.; Guzei, I. A.; Espenson, J. H. *Inorg. Chem* **1999**, *38*, 3762−3763. Lente, G.; Guzei, I. A.; Espenson, J. H. *Inorg. Chem* **2000**, *39*, 1311−1319.

(5) Li, M.; Ellern, A.; Espenson, J. H. *Inorg. Chem* **2005**, *44*, 3690−3699.

10.1021/ja0519334 CCC: $30.25

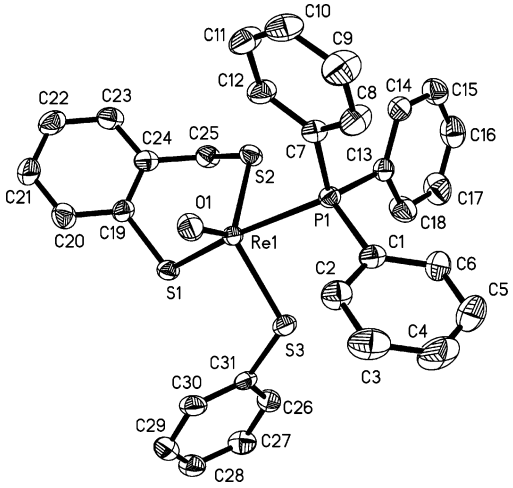

Figure 1. ORTEP diagram of **1a** with thermal ellipsoids drawn to 50% probability.

Chart 1

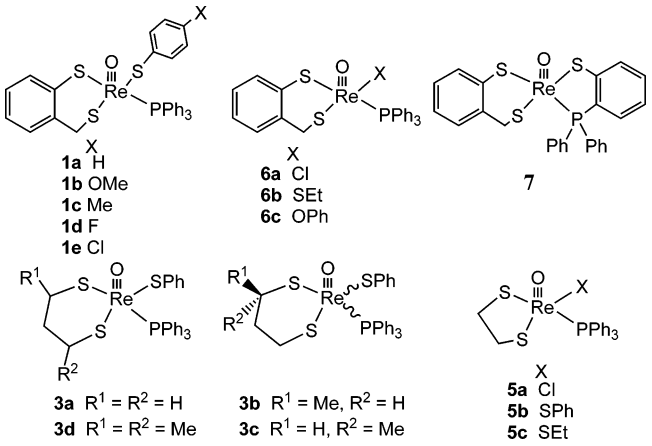

Scheme 1

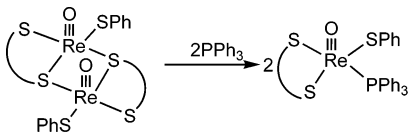

S-loop-S = mtp, edt, pdt, pdtMe, and $pdtMe_2$

because monomerization proceeds much more readily than the C−S bond cleavage reactions. With dt = pdt, pdtMe, and $pdtMe_2$, however, mixtures of monomers were obtained due to stereoisomers and the competing formation of C−S cleavage products; no attempts were made to isolate the monomers.

The structure of **1a** in the solid state was determined by X-ray crystallography. An ORTEP diagram is shown in Figure 1, and selected bond lengths and angles are listed in Table 1. The structure is very close to that of its analogue, [MeReO(mtp)-(PPh_3)], **9**. The dithiolate ligand in **1a** is bound asymmetrically with Re−S1 = 233.46(10) pm and Re−S2 = 228.44(10) pm; the Re−O distance is 169.3(3) pm. These distances are comparable to those found in **9**, for which the three respective bond distances are 234.0, 227.54, and 169.6 pm.[6]

The monomerization reaction (Scheme 1) was used to prepare the $Re^{V}O$ complexes with various phosphines. Room-temperature syntheses of $[ClReO(dt)(PPh_3)]$ with dt = edt (**5a)** and mtp (**6a**) were developed. The method proved to be useful for preparing precursors to a variety of complexes with different ancillary ligand environments. Reactions of $[Cl_3ReO(PPh_3)_2]$ and 1.0 equiv of edt or mtp in toluene afford products **5a** and **6a**, respectively.

$$[Cl_3ReO(PPh_3)_2] + dtH_2 \rightarrow [ClReO(dt)(PPh_3)] + PPh_3 + 2HCl \quad (dt = edt, mtp) \quad (4)$$

The ^1H and ^{31}P NMR spectra and the elemental analyses are consistent with the given formulas. Further evidence comes from the single-crystal X-ray structures. The ORTEP diagrams of the molecular structures are shown in Figure 2. These square-pyramidal molecules resemble **1a**, with Re−Cl distances of 234.29(19) and 232.62(18) pm for **5a** and **6a**, respectively, which are similar to those in related Re(V) dithiolate complexes.[7] The chloride ion is positioned trans to the benzylic sulfur atom. Attempts to synthesize $[ClReO(dt)(PPh_3)]$ (dtH_2 = $pdtH_2$, 1,2-benzenedimethanethiol, and 1,4-butanedithiol) by a similar procedure were unsuccessful.

With **5a** and **6a** in hand, substitution reactions with ancillary ligands were examined. Treatment of **6a** with 1.0 equiv of $LiSC_6H_4$-*p*-X (X = OMe, Me, F, Cl) gave **1a**−**e** as green solids in 51−68% yields (Scheme 2). The ^1H NMR spectra of these complexes display very similar resonance patterns; their ^{31}P NMR spectra show a singlet at 18.7 ± 0.1 ppm.

Treatment of **6a** with 1.0 equiv of the chelating ligand lithium 2-(diphenylphosphino)benzenethiolate in benzene resulted in displacement of PPh_3 and formation of **7** (Scheme 2). Its ^{31}P NMR spectrum exhibits a singlet at δ 55.9 ppm. The structure of **7** was confirmed by X-ray diffraction (Figure 3); selected distances and angles are given in Table 1. The coordination geometry about rhenium is square-pyramidal, with a Re−O length of 168.6(5) pm and Re−S bond lengths in the range of 227.89(18)−235.1(2) pm. The aryl ring of the chelating ligand *o*-$SC_6H_4PPh_2$ is nearly coplanar with the P1−Re−S3 plane: the dihedral angle is 13.9°. The distances between rhenium and its donor atoms are only slightly affected, as can be seen from a comparison of the structures of **1a** and **7**.

Addition of 1.0 equiv of $LiSC_2H_5$ to **6a** followed by workup afforded **6b** as a green solid. The ^1H NMR spectrum established the presence of an ethyl group in which the CH_3 protons appeared at δ 1.45 and the chemically inequivalent CH_2 protons appeared as doublets of quintets at δ 3.86 and 3.69. A suitable crystal was obtained by vapor diffusion of hexane into a CH_2-Cl_2 solution of the complex. The significant bond lengths and angles are listed in Table 1; an ORTEP diagram is shown in Figure 3. Treatment of **6a** with 1.0 equiv of LiOPh in anaerobic THF led to the desired product (Scheme 2). The salient feature in the ^1H NMR spectrum of **6c** is the appearance of the methylene protons at δ 4.77 and 3.37, upshifted in comparison with **6a**; the ^{31}P resonance shifts from δ 23.0 (**6a**) to 32.5 ppm (**6c**). In a similar manner, treatment of **5a** with $LiSC_2H_5$ at room temperature gave $[EtSReO(edt)(PPh_3)]$, **5c**, after 3 h.

(6) Jacob, J.; Guzei, I. A.; Espenson, J. H. *Inorg. Chem.* **1999**, *38*, 1040−1041.

(7) Gangopadhyay, J.; Sengupta, S.; Bhattacharyya, S.; Chakraborty, I.; Chakravorty, A. *Inorg. Chem* **2002**, *41*, 2616−2622. Dirghangi, B. K.; Menon, M.; Pramanik, A.; Chakravorty, A. *Inorg. Chem.* **1997**, *36*, 1095−1101.

Table 1. Selected Bond Lengths (pm) and Angles (deg)

	1a	5a[b]	6a	6b	7	9[c]
Re−O	169.3(3)	169.3(5)	167.5(5)	168.8(4)	168.6(5)	169.6(5)
Re−S_{Ph}[a]	233.46(10)	228.8(2)	231.7(2)	233.0(2)	235.1(2)	234.0(2)
Re−S_{Bn}[a]	228.44(10)	225.30(19)	223.73(19)	228.06(18)	227.89(18)	227.54(19)
Re−X[a]	230.09(10)	234.29(19)	232.62(18)	2.270(2)	230.79(18)	213.1(7)
Re−P	249.81(10)	247.99(17)	248.68(18)	247.86(17)	243.63(18)	244.68(19)
O−Re−S_{Ph}[a]	105.78(10)	108.63(17)	104.95(19)	105.48(17)	106.15 (19)	109.06(19)
O−Re−S_{Bn}[a]	119.21(10)	113.7(2)	114.3(2)	117.9(2)	115.03(18)	116.14(19)
O−Re−P	92.10(10)	99.47(17)	92.87(19)	92.11(17)	98.96(18)	100.13(18)
O−Re−X	113.99(10)	111.9(2)	120.9(2)	115.2(2)	113.68(18)	112.1(3)

[a] S_{Ph} is bound to the phenyl of mtp; S_{Bn} is the benzylic S, bound to the methylene group of mtp; X = Cl for **6a** and **5a**; X = S for **1a**, **6b**, and **7**; and X = C for **9**. [b] Both S_{Ph} and S_{Bn} refer to the edt ligand. [c] Data from one of two independent molecules; ref 6.

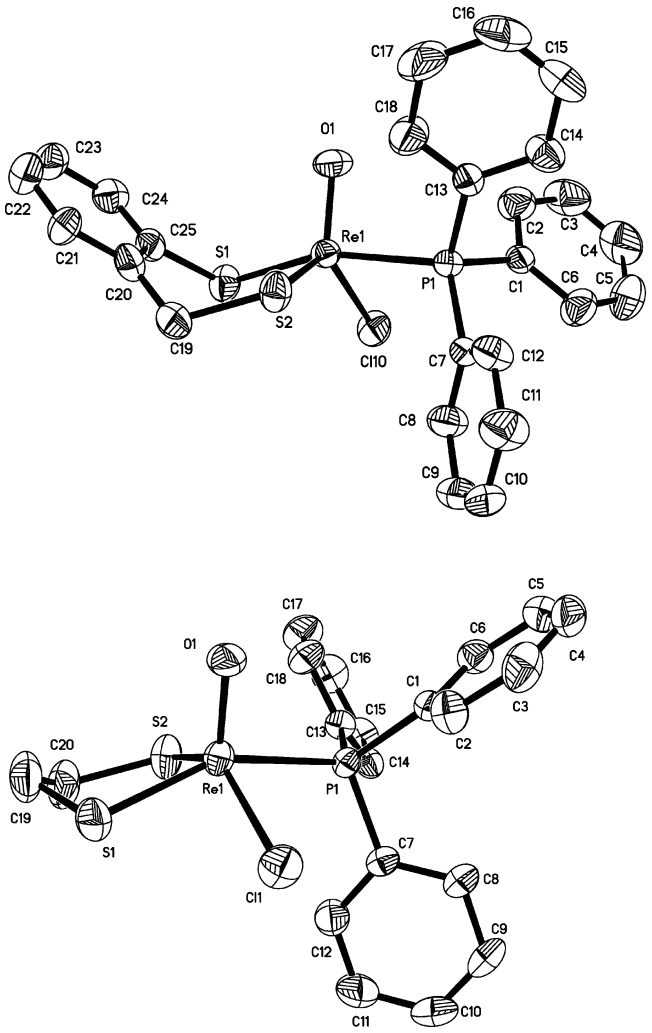

Figure 2. ORTEP diagrams for **5a** and **6a** with thermal ellipsoids drawn to 50% probability.

Reactions of the mtp Complexes 1a−e with PPh_3. As reported previously, treatment of **1a** with excess PPh_3 leads to the metalacyclic Re(V) complex **2a**, eq 1. Similarly, C−S bond cleavage reactions also occur for $[XC_6H_4SReO(mtp)(PPh_3)]$ (**1b−e**, X = OMe, Me, F, Cl). These reactions were confirmed by ^1H and ^{31}P NMR spectra. Products **2b−e** show NMR patterns quite similar to that of **2a**. The ^1H NMR resonances of the methylene group of the mtp ligand of each product are downshifted in comparison with those of the corresponding reactants; the ^{31}P NMR spectra exhibit resonances around δ 35.0.

Treatment of **6b** with excess PPh_3 in benzene at room temperature allowed the isolation of **8** as a red-brown solid in low yield after column chromatography. Examination of the

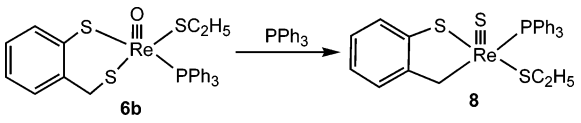

entire reaction mixture by ^1H NMR in C_6D_6 revealed that the conversion of **6b** to **8** proceeded quantitatively, although the isolated yield was lower owing to decomposition on the chromatographic column. The ^1H and ^{31}P NMR spectra of **8** are consistent with the C−S bond rupture at the position trans to the ethanethiolate ligand. In particular, the δ 4.92 doublets of doublets ($^4J_{P-H}$ = 1.2 and $^2J_{H-H}$ = 12 Hz) and the δ 3.35 doublet ($^2J_{H-H}$ = 12 Hz), assigned as the methylene protons of the benzylic moiety in the ^1H NMR spectrum of **6b**, are replaced by δ 6.67 ($^3J_{P-H}$ = 3.2 and $^2J_{H-H}$ = 16.6 Hz) and δ 4.09 ($^3J_{P-H}$ = 9.6 and $^2J_{H-H}$ = 16.6 Hz) doublets of doublets. Accordingly, the chemical shifts of the ethyl protons are slightly changed, although two sets of multiplets of the methylene protons of the ethyl group are collapsed to one set.

Reactions of **6a**, **6c**, and **7** with PPh_3 were monitored by ^1H and ^{31}P NMR spectra in C_6D_6. Neither a C−S cleaving reaction nor a triphenylphosphine oxide adduct of rhenium was observed, even upon prolonged reaction time or heating. It should be mentioned that the phosphorus resonance of **6a**, upon addition of excess PPh_3, broadens without changing its chemical shift, presumably due to PPh_3 exchange.

Reactions of pdt Complexes with PPh_3. In reactions of the Re(V) complexes with an mtp ligand, **1a−e**, C−S bond cleavage occurred *only* at the benzylic moiety. To learn whether this is intrinsic or due to the mtp ligand, complexes with pdt were prepared. Treatment of **3a** with PPh_3 yields the thoroughly characterized C−S cleavage product **4a**. Its formation does not allow a distinction to be made as to the position of C−S bond scission, owing to the symmetry of the pdt ligand. Thus we

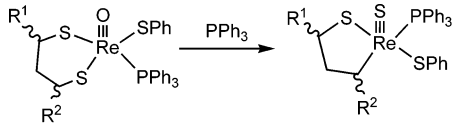

examined the reactions of asymmetric pdt isomers with PPh_3. Reaction of 1,3-butanedithiol (pdtMe) with $\{(ReO)(SPh)_3\}_2$[5] in a ratio of 2:1 should, in principle, afford the three dimeric stereoisomers shown in Chart 2.

Scheme 2

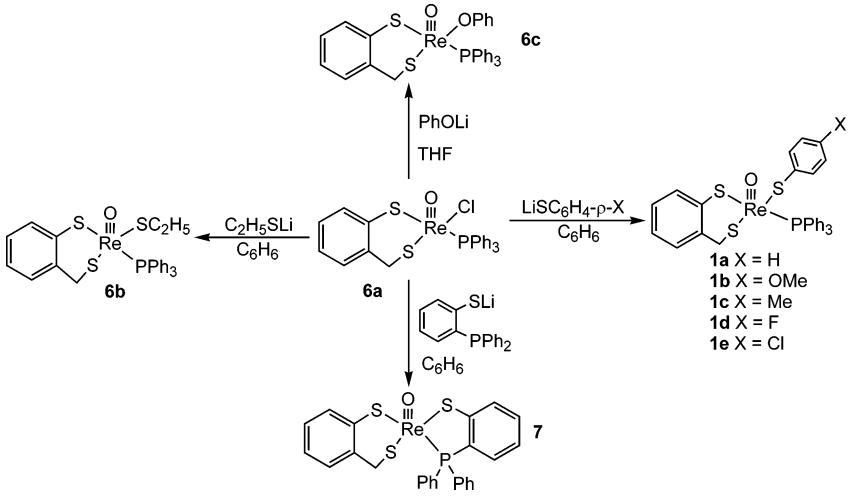

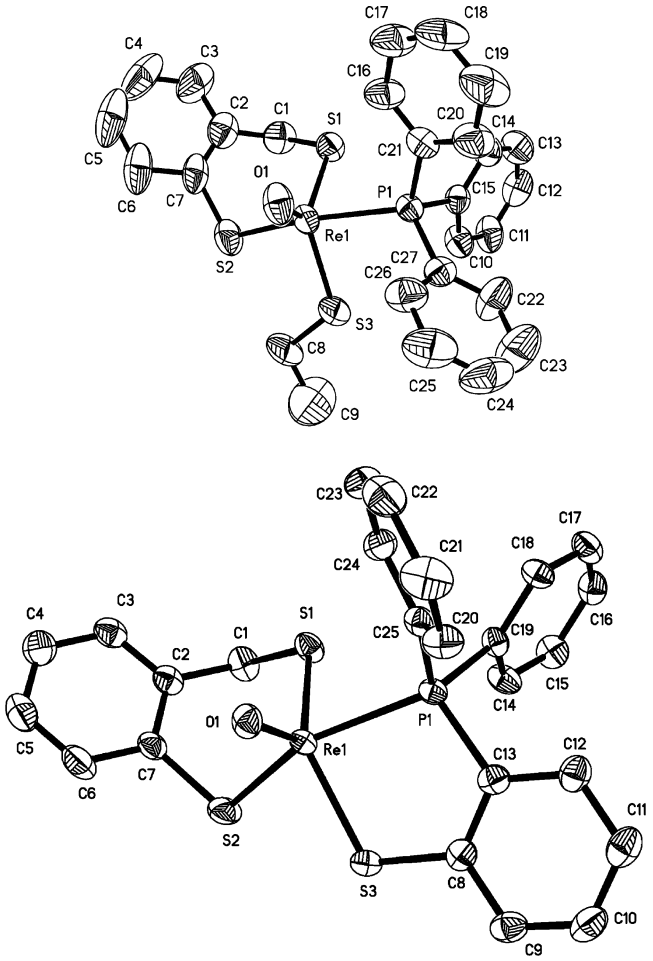

Figure 3. ORTEP diagrams for **6b** and **7** with thermal ellipsoids drawn to 50% probability.

According to the ^{1}H NMR spectra of the dimers used in the C−S cleaving reaction, the ratio of methyl groups pointing toward the Re≡O bond to those pointing away from that bond is 3.37:1. Two well-resolved sets of proton and phosphorus resonances of unequal intensity were observed in the NMR spectra of the C−S cleaved products in C_6D_6. The proton resonances were correlated by a 2D COSY spectrum (Figure S1, Supporting Information); the phosphorus resonances appear at δ 31.8 and 32.3 for **4b** and **4c**, respectively. Integration of

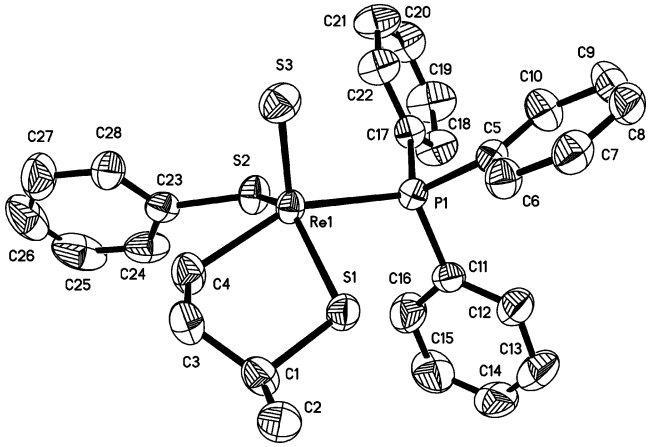

Figure 4. ORTEP diagram for **4b** with thermal ellipsoids drawn to 50% probability. Selected distances (pm) and bonding angles (°): Re(1)−S(3), 208.99(10); Re(1)−C(4), 214.6(4); Re(1)−S(1), 226.88(9); Re(1)−S(2), 228.57(9); Re(1)−P(1), 244.00(8); S(3)−Re(1)−C(4), 107.75(11); S(3)−Re(1)−S(1), 117.55(4); C(4)−Re(1)−S(1), 79.43(10); S(3)−Re(1)−S(2); 112.97(4); C(4)−Re(1)−S(2), 88.01(10); S(3)−Re(1)−P(1), 101.75(4); S(1)−Re(1)−P(1), 84.27(3); S(2)−Re(1)−P(1), 84.27(3).

Chart 2

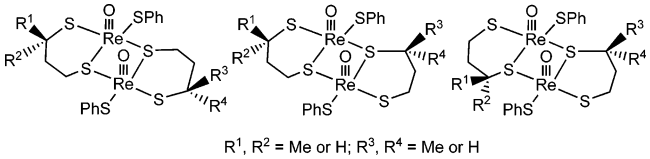

the CH_3 resonances affords a ratio of 3.26:1, which is in excellent agreement with that of the reactants. The identities of isomers **4b** (major) and **4c** were assigned on the basis of 2D COSY and HMQC C−H correlation spectra.

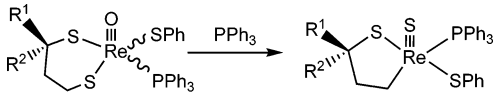

The structure of **4b** was confirmed by X-ray diffraction; the ORTEP diagram and significant bond lengths and angles are shown in Figure 4. The methyl group lies on the same side of

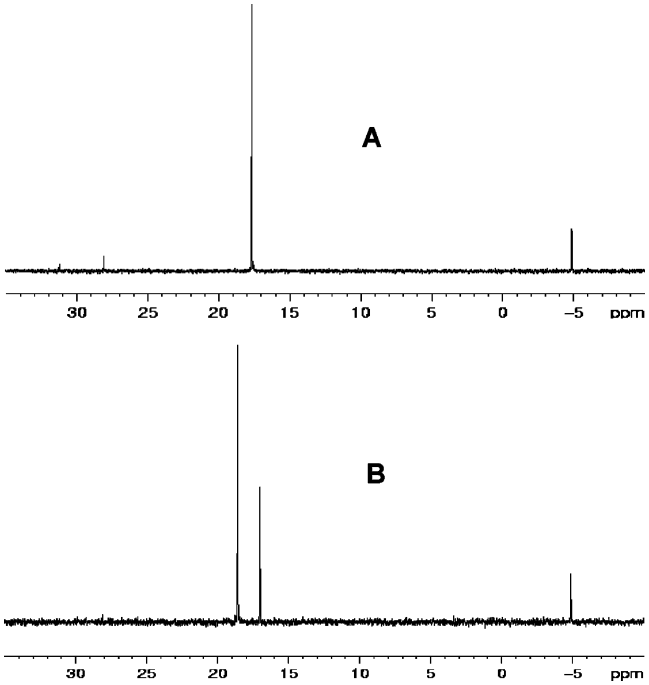

Figure 5. ^{31}P NMR spectra of monomerization of the dimers with pdt (A) and mtp (B) ligands with PPh_3 in CD_2Cl_2.

the molecule as the sulfide−rhenium bond; the Re≡O distance is 208.99(10) pm. The Re−C bond distance in **4b** is 214.6(4) pm, comparable to those found in **4a** and other related Re(V)−S complexes.[8]

To learn whether C−S bond scission is regioselective, the monomerization of dimers with mtp, pdt, and pdtMe ligands was monitored in a 1:2$^+$ ratio of dimer to PPh_3 by ^1H and ^{31}P NMR spectroscopy in CD_2Cl_2. For the dimer with a pdt ligand, one intensified resonance at 17.7 ppm assignable to **3a** was observed in the ^{31}P NMR spectra in Figure 5A, in addition to **4a** at 31.2 ppm, free PPh_3 at −4.8 ppm, and Ph_3PO at 28.1 ppm. Unexpectedly, two monomeric isomers with the mtp ligand were detected as shown in Figure 5B. The resonance due to **1a** appears at 18.6 ppm and that due to **1a′** at 17.0 ppm; moreover, isomer **1a′** was converted rapidly to **1a** by PPh_3 catalysis.[3]

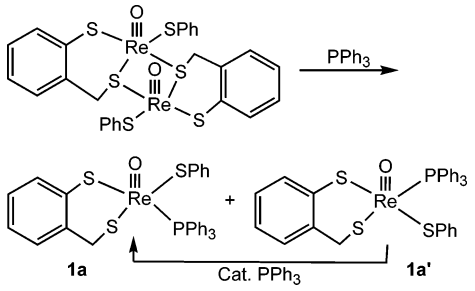

In monomerization of the dimer with the pdtMe ligand, two pairs of resonances with roughly equal intensity were observed; those at 17.4 and 16.8 ppm were assigned to **3b** and **3b′** and those at 17.1 and 15.6 ppm to **3c** and **3c′**. In contrast to the case with the mtp ligand, no interconversion between **3b** and **3b′**, or between **3c** and **3c′**, was observed, even in a 1:12 ratio of the dimer to PPh_3 (Figure 6). As the reaction proceeded, the

(8) Jacob, J.; Guzei, I. A.; Espenson, J. H. *Inorg. Chem.* **1999**, *38*, 3266−3267.

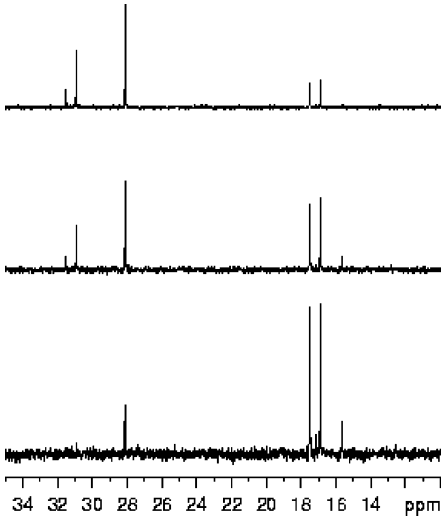

Figure 6. Variation of ^{31}P NMR spectra with time in CD_2Cl_2 for monomerization of the dimer with the pdtMe ligand (6.5 mM) with PPh_3 (77 mM): 15 min (bottom), 2 h (middle), and 4 h (top).

isomers **3b**/**3b′** and **3c**/**3c′** disappeared to form *only* **4b** (δ 30.9 ppm) and **4c** (δ 31.5 ppm), respectively. The results show clearly that the C−S cleavage is not regioselective.

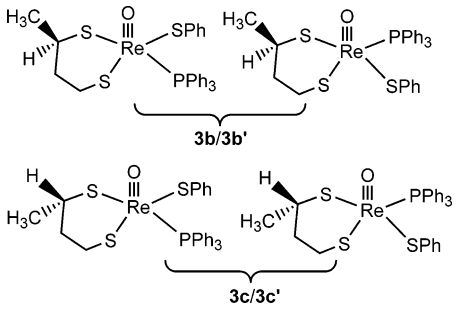

The difference in monomerization with asymmetric mtp and pdtMe can perhaps be attributed to the coordination abilities of the thiolato donors. In mtp, the sulfur atom directly connected to the phenyl ring coordinates to the rhenium center less strongly than the sulfur atom connected to the methylene group. This favors formation of the thermodynamic isomer **1a**. Both sulfur atoms in pdt have the same coordination abilities, and this system lacks a driving force for isomer interconversion.

Reactions of edt Complexes with PPh_3. C−S bond activation occurs selectively at the six-membered rings with the mtp and pdt ligands as shown above, which results in the formation of stable five-membered rings. To extend the reactions further and to examine their selectivity, the geometrically constrained complex [EtSReO(edt)(PPh_3)], **5c**, was used for reaction with PPh_3. The process was investigated by ^1H and ^{31}P NMR spectroscopy. As it happens, no reaction was observed.

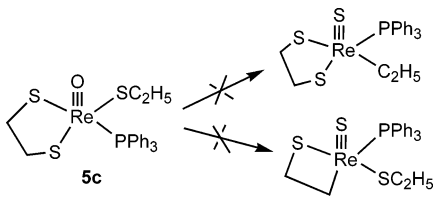

Kinetics of the C−S Cleavage Reactions. These reactions were monitored by their UV−visible spectroscopic changes. The

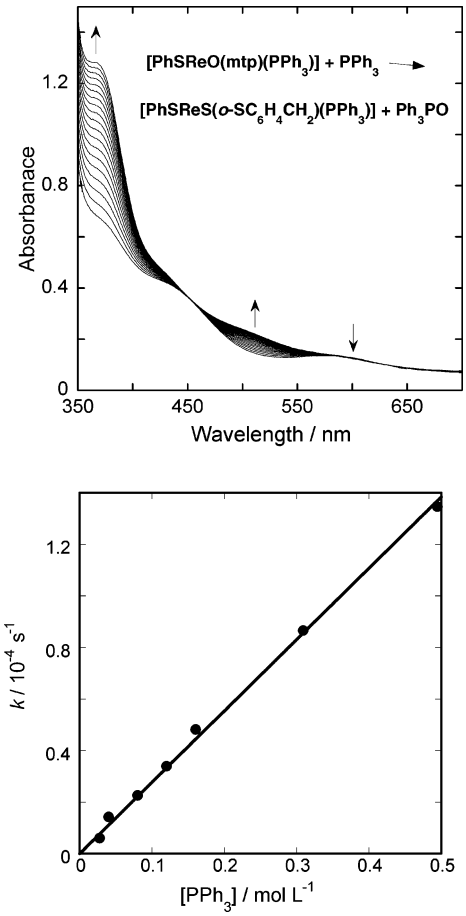

Figure 7. (Top) Changes in the UV−visible spectrum observed during the reaction of **1a** with PPh_3. The respective initial concentrations of **1a** and PPh_3 were 1.26×10^{-4} and 0.329 mol L^{-1}. The spectra were recorded at 25 °C at 10.0 min intervals. (Bottom) Plot of k_{obs} against the concentration of PPh_3.

time course of the reaction between **1a** and PPh_3 is depicted in Figure 7; the tight isosbestic points show that the reaction progresses to the product without intermediates building up to concentrations that contribute appreciably to the spectral changes. The final spectrum is identical with that of **2a** measured separately. Global fitting of the spectra (350−650 nm) with SpecFit[9] establishes that the reaction follows pseudo-first-order kinetics at all of these wavelengths under these conditions. Values of the first-order rate constants proved to be independent of the initial concentration of the Re(V) complexes, with k_{obs} linearly dependent on [PAr_3] (Figure 7 and Supporting Information). All reactions adhere to the second-order rate law,

$$-\frac{\mathrm{d[Re(V)]}}{\mathrm{d}t} = k_2[\mathrm{Re(V)}][\mathrm{PAr_3}]$$

Rate constants are listed in Table 2. To explore the independent effects of the phosphine coordinated to **1a** and of the external phosphine that attacks it, several variations were carried out. The reaction between **1a** and P(C_6H_4-*p*-OMe)$_3$ gave $k_2 = 2.37(4) \times 10^{-4}$ L mol^{-1} s^{-1}, whereas that between an analogue of **1a**, [PhSReO(mtp)P(C_6H_4-*p*-OMe)$_3$], and P(C_6H_4-*p*-OMe)$_3$ has $k_2 = 2.23(3) \times 10^{-4}$ L mol^{-1} s^{-1}. Furthermore, the reaction between **1a** and P(C_6H_4-*p*-CF_3)$_3$ has $k_2 = 2.78(6) \times 10^{-4}$ L mol^{-1} s^{-1}, comparable to that between **1a** and PPh_3. These data demonstrate that the rate constants are insensitive to the substituents (Y) in P(Ph-*p*-Y)$_3$ (Y = H, MeO, CF_3).

On the other hand, the reactions between [(C_6H_4-*p*-X)SReO(mtp)(PPh_3)] (X = MeO, Me, H, F, Cl) and PPh_3 are accelerated by an electron-withdrawing group, whereas an electron-donating group has the opposite effect. A plot of log k_2 vs the Hammett substituent constant (σ) is presented in Figure 8; analysis of the data, excluding the point for MeO, gives a slope $\rho = 0.66$. Clearly, the point for X = MeO lies off the line. This substituent is the most strongly electron-withdrawing. Aside from noting the fact, however, we offer no explanation for the unusual behavior.

The rate constants also vary with changes of dithiolate ligands. In a series of complexes with various pdt ligands, the rates decrease with increasing numbers of methyl groups on the pdt framework. A plot of log k_2 vs numbers of the methyl group exhibits a good linear correlation ($R = 0.97$, Figure S8, Supporting Information).

Infrared Spectra and Electrochemistry. The infrared spectra of the complexes (KBr disk) show the characteristic of Re≡O band, ranging from 978 to 947 cm^{-1}. These values are within the range for the Re≡O stretching frequencies reported in the literature.[7,10]

Cyclic voltammetry was used to investigate the electrochemical behavior of the complexes, with results as summarized in Table 3. Compound **7** exhibited a reversible one-electron reduction; the others displayed quasi-reversible or irreversible voltammograms (see Supporting Information). Comparison of the reduction potentials in a series of mtp complexes indicates that the potentials increase in the order OPh < Me < PhS ≈ EtS ≈ Cl ≈ chelating ligand, *o*-$SC_6H_4PPh_2$. This trend shows that the potentials are sensitive to the nature of the ancillary ligand. Compound **5b**, with a five-membered ring, is difficult to reduce.

Discussion

Electronic Factors. It has been well-documented that the $Re^{V}O$ moiety undergoes oxygen atom transfer upon reduction of Re(V) to Re(III), the transfer process being initiated by nucleophilic substrate attack on the π^* ReO orbital.[11,12] A difference in the electron-donating abilities of the ligands is expected to influence the reactivity dramatically. Electron-withdrawing ArS ligands facilitate nucleophilic attack, opposite to the effect of electron-rich ligands. For the reactions between **1a** and a series of para-substituted phosphines, P(Ph-*p*-Y)$_3$ (Y = H, MeO, CF_3), the rate reaction constants are nearly but not precisely the same (Table 3).

The kinetic data raise two issues. First, note the identity (within three standard deviations) of the values of k_2 for reactions when P(C_6H_4-*p*-OMe)$_3$ is the attacking phosphine. Phosphine exchange between **1a** and free phosphine occurs[3] prior to C−S bond cleavage, as evidenced by the ^{31}P NMR spectra. The C−S cleavage step with PAr_3 is thus a single reaction between [PhSReO(mtp)P(C_6H_4-*p*-OMe)$_3$] and P(C_6H_4-*p*-OMe)$_3$.

(9) Binstead, R. A.; Zuberbuhler, A. D.; Jung, B. *SPECFIT*, Global analysis system; Spectrum Software Associates, 1993−2003.

(10) Parachristou, M.; Pirmettis, I. C.; Tsoukalas, C.; Papagiannopoulou, D.; Raptopoulou, C.; Terzis, A.; Stassinopoulou, C. I.; Chiotellis, E.; Pelecanou, M.; Papadopoulos, M. *Inorg. Chem* **2003**, *42*, 5778−5784.

(11) Holm, R. H. *Chem. Rev.* **1987**, *87*, 1401−1449. Mayer, J. M. *Adv. Trans. Met. Coord. Chem.* **1996**, *1*, 105−157.

(12) Nugent, W. A.; Mayer, J. M. *Metal−Ligand Multiple Bonds*; John Wiley & Sons: New York, 1988.

Table 2. Summary of the Rate Constants for Reactions between Oxorhenium(V) Dithiolates and Triarylphosphines in C_6H_6 at 25 °C

[PhSReO(mtp)(PPh$_3$)] + P(Ar-*p*-Y)$_3$		[(Ar-*p*-X)SReO(mtp)(PPh$_3$)] + PPh$_3$		[PhSReO(dt)(PPh$_3$)] + PPh$_3$	
Y	k_2 (L mol^{-1} s^{-1})	X	k_2 (L mol^{-1} s^{-1})	dt	k_2 (L mol^{-1} s^{-1})
H	$2.77(4) \times 10^{-4}$	MeO	$2.70(7) \times 10^{-4}$	pdt	$3.61(2) \times 10^{-3}$
MeO	$2.37(4) \times 10^{-4}$	Me	$2.18(4) \times 10^{-4}$	pdtMe	$2.27(4) \times 10^{-3}$
CF_3	$2.78(6) \times 10^{-4}$	H	$2.77(4) \times 10^{-4}$	pdtMe$_2$	$7.7(5) \times 10^{-4}$
	$2.23(3) \times 10^{-4}$ [a]	F	$3.31(7) \times 10^{-4}$		
	$2.69(7) \times 10^{-4}$ [b]	Cl	$3.96(6) \times 10^{-4}$		

[a] For [PhSReO(mtp)P(C_6H_4-*p*-OMe)$_3$] and P(C_6H_4-*p*-OMe)$_3$. [b] For [EtSReO(mtp)(PPh$_3$)] and PPh$_3$.

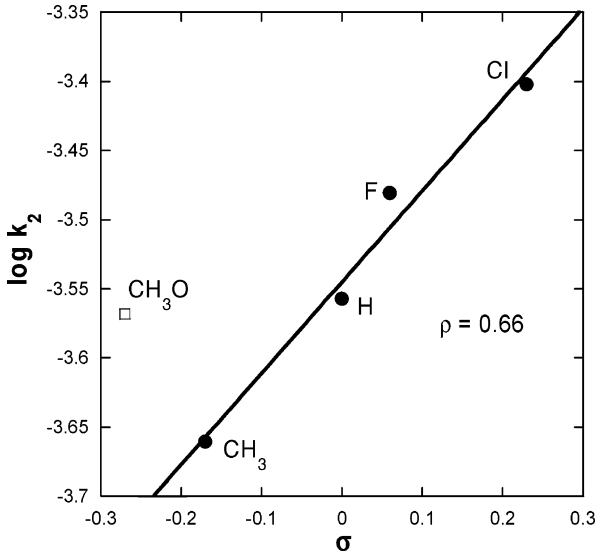

Figure 8. Plot of log k_2 against the Hammett constant σ for reactions between [(C_6H_4-*p*-XS)ReO(mtp)(PPh$_3$)] and PPh$_3$.

Table 3. Electrochemical Data for Reduction of the Oxorhenium(V) Complexes[a]

complex	$E_{p,c}$ (V)	complex	$E_{p,c}$ (V)
6a	−0.84	**3a**	−1.10
7	−0.90	**9**	−1.23
1a	−0.95	**5b**	(−1.25)[b]
6b	−1.04	**6c**	(−1.49) [b]

[a] Potentials in CH_2Cl_2 referenced vs SCE. [b] Irreversible.

The second issue is more troubling. The inductive effects of the two phosphines in the transition state appear nearly to cancel one another. It is reasonable to assert that a key step is the attack of phosphine at the oxo group of **1a**. Studies have amply verified this mode of attack on metal-oxo groups.[13] Given that, the phosphine attacking **1a** acts as a nucleophile, and for it the rate constants for P(C_6H_4X)$_3$ can reasonably be expected to follow the sequence X = MeO > H > CF_3. Indeed, a strong inductive effect can be expected, because of data pertaining to reaction 1, for which a Hammett correlation gave the reaction constant $\rho = -0.70$.[1414]

$$[MeRe^{VII}O_2(mtp)] + PAr_3 \rightarrow [MeRe^{V}O(mtp)(OPAr_3)] \quad (5)$$

On the other hand, the ring substituent on the phosphine already coordinated to the rhenium atom should exert just the opposite inductive effect. It appears that the opposing inductive effects nearly cancel one another; compare these values of k_2/10^{-4} L mol^{-1} s^{-1}: 2.37 (MeO), 2.77 (H), and 2.78 (CF_3). This is not unreasonable, given that the two phosphines exert their opposite inductive effects in the same transition state.

Mechanism. To probe the mechanistic features of the C−S bond-cleaving process, the reaction between **1a** and PPh$_3$ was examined in detail by ^{1}H and ^{31}P NMR spectra in C_6D_6 on the basis of its simplified ^{1}H NMR spectroscopy in the aliphatic region. The variable spectra with time are shown in Figure 9. Three well-resolved pairs of resonances are observed in ^{1}H NMR spectrum; their correlation is evident in the 2D COSY spectrum. The protons (H_s and H_s') are present as the doublet peaks at δ 4.70 and 3.43 of **1a**, which then disappeared as the reaction progressed. The δ 6.29 and 4.11 (H_p and H_p') resonances were assigned to **2a**, which builds up at the expense of **1a**. The phosphorus signals are found at δ 19.0 for **1a** and at δ 34.8 for **2a**; a singlet at δ 25.9 ppm is due to Ph$_3$PO, as confirmed by an authentic sample. Two doublets in the ^{1}H spectrum at δ 4.95 and 3.71 (H_I and H_I') were assigned to an intermediate, which increased and then disappeared. At most it amounted to ca.12%. No obvious Re−^{31}P resonance appeared in the ^{31}P spectra, although a minor transient resonance near δ 35 (the Re−^{31}P resonance of the product) cannot be discounted.

Therefore, four possible intermediates have to be considered. A three-coordinate species **A** can be ruled out due to a splitting ($\Delta\delta$ = 1.3) in chemical shifts of the methylene protons. It is possible but unreasonable that dimeric isomers **B** and **C** are present in solution. An analogue, {ReO(bdt)(SPh)}$_2$ (bdt = *o*-benzenedithiol), reacted with PPh$_3$ very rapidly,[5] suggesting that, in the presence of excess PPh$_3$, it would be impossible to detect the dimers **B** and **C** by ^{1}H NMR. It is also expected that the extent of dimer formation would be very small with phosphine present in such large excess. On the basis of the observed inequivalent protons of the methylene group due to the anisotropic effect of the Re≡S core,[15] and the absence of H−P coupling, the coordinatively unsaturated intermediate **D′** is being proposed. The chemical conclusions are, however, considerably more consistent with earlier studies of Re(V) chemistry if structure **D**, and not **D′**, is assigned to the intermediate, as shown in Chart 3.

The data from this study and from earlier work allow us to assign a plausible multistep mechanism. As demonstrated experimentally, phosphine exchange occurs prior to the main reaction. Studies of [MeReO(dt)PR$_3$] systems show that exchange occurs sequentially, via double turnstile rotation processes as shown in Scheme 3. Note that intermediate **I** increases to a concentration where it can easily be detected.[3]

(13) Seymore, S. B.; Brown, S. N. *Inorg. Chem* **2000**, *39*, 325−332. Smith, P. D.; Millar, A. J.; Young, C. G.; Ghosh, A.; Basu, P. *J. Am. Chem. Soc.* **2000**, *122*, 9298−9299. Nemykin, V. N.; Davie, S. R.; Mondal, S.; Rubie, N.; Kirk, M. L.; Somogyi, A.; Basu, P. *J. Am. Chem. Soc.* **2002**, *124*, 756−757. Basu, P.; Nemykin, V. N.; Sengar, R. S. *Inorg. Chem* **2003**, *42*, 7489−7501.

(14) Wang, Y.; Espenson, J. H. *Inorg. Chem* **2002**, *41*, 2266−2274.

(15) Martin, D.; Piera, C.; Mazzi, U.; Rossin, R.; Solans, X.; Font-Bardia, M.; Suades, J. *J. Chem. Soc., Dalton Trans.* **2003**, 3041−3045. Papadopoulos, M. S.; Pirmettis, I. C.; Pelecanou, M.; Raptopoulou, C. P.; Terzis, A.; Stassinopoulou, C. I.; Chiotellis, E. *Inorg. Chem.* **1996**, *35*, 7377−7383.

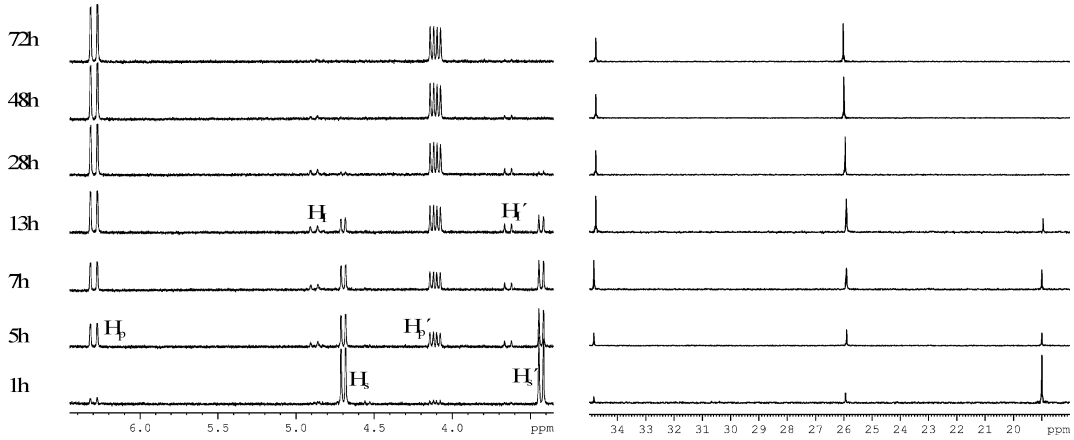

Figure 9. Variation of ^{1}H and ^{31}P NMR spectra with time in C_6D_6 for reaction of **1a** (9.4 mM) and PPh_3 (0.16 mol L^{-1}) at 25 °C.

Chart 3. Structural Formulas of Possible Intermediates

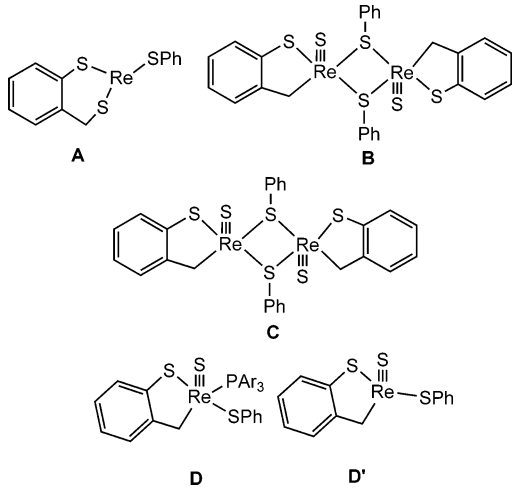

Scheme 3

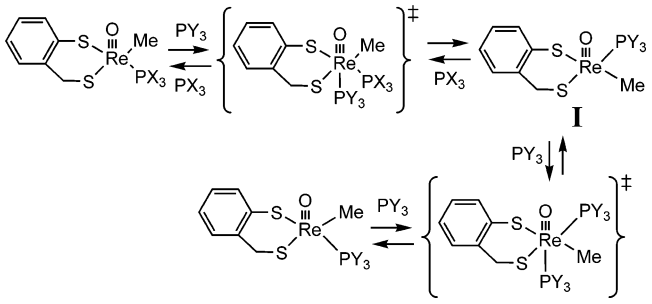

Scheme 4. Suggested Mechanism of C–S Cleavage

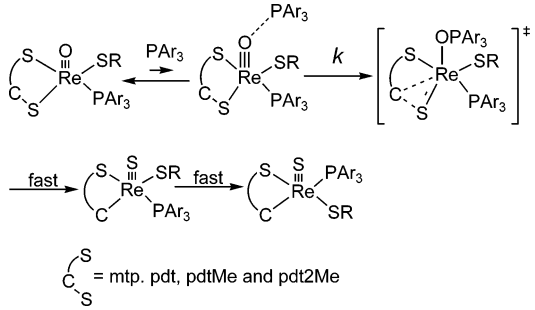

The suggested route to C–S cleavage is presented in Scheme 4. Following phosphine exchange, PAr_3 attacks nucleophilically at the oxygen atom of $Re^{V}O$ in the rate-controlling step, which affords a phosphine oxide complex of Re(III). In the transition state, a [1,2] migration of an alkyl group to rhenium is proposed. Events following formation of the transition state are speculative, of course, but we suggest that weakly coordinating Ar_3PO is lost first, yielding **D**. Finally, **D** isomerizes to the final product **2**. This, too, occurs by a turnstile rotation sequence analogous to that in Scheme 3.

Recently, Mayer and co-workers have reported the rhenium(V) complexes $(HBpz_3)ReO(R)Cl$ ($HBpz_3$ = hydrotris(1-pyrazolyl)borate, R = aryl, ethyl) undergo photochemical metal-to-oxo migrations to form rhenium(III) alkoxides.[16] Analogous migrations to terminal imido or sulfide complexes have also been proposed.[17]

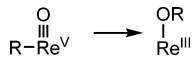

However, the reverse reaction, rearrangement of an alkoxide to an oxo-alkyl, is rare.[18] In the present cases, migration of alkanethiolate to form the alkylthiolato complex, to our knowledge, is unprecedented.

Reactivity. The complexes with the Re≡O core exhibit a wide range of reactivity toward PPh_3. The compounds [XReO(dt)(PPh_3)] (X = SPh or SEt; dt = mtp or pdt) react with PPh_3 to induce C–S activation. At other end of the spectrum are the complexes which show no analogous reaction. These include [XReO(mtp)(PPh_3)] (X = OPh, Me, Cl, and *o*-$SC_6H_4PPh_2$) and [YReO(edt)(PPh_3)] (Y = SPh and SEt). A few examples of $Re^{V}O$ and $Tc^{V}O$ complexes possessing a sulfur donor set can be reduced by PPh_3 to form deoxygenated, stable Re(III) and Tc(III) phosphine adducts instead.[19]

The electrophilicity of the multiply bonded ligand is in large part controlled by the energy and character of the LUMO.[12,20] The E_{pc} values, lying between −0.84 and −1.49 V (Table 3),

(16) Brown, S. N.; Mayer, J. M. *J. Am. Chem. Soc.* **1994**, *116*, 2219–2220. Brown, S. N.; Mayer, J. M. *Organometallics* **1995**, *14*, 2951–2960.
(17) Nugent, W. A.; Harlow, R. L. *J. Am. Chem. Soc.* **1980**, *102*, 1759–1760. Vivanco, M.; Ruiz, J.; Floriani, C.; Chiesi-Villa, A.; Rizzoli, C. *Organometallics* **1993**, *12*, 1802–1810.
(18) Asselt, A. v.; Burger, B. J.; Gibson, V. C.; Bercaw, J. E. *J. Am. Chem. Soc.* **1986**, *108*, 5347–5349. Nelson, J. E.; Parkin, G.; Bercaw, J. E. *Organometallics* **1992**, *11*, 2181–2189. Tahmassebi, S. K.; Conry, R. R.; Mayer, J. M. *J. Am. Chem. Soc.* **1993**, *115*, 7553–7554.
(19) Dilworth, J. R.; Neaves, B. D.; Hutchinson, J. R.; Zubieta, J. A. *Inorg. Chim. Acta* **1982**, *65*, L223–L224. Davison, A.; Vries, N. D.; Dewan, J.; Jones, A. G. *Inorg. Chim. Acta* **1986**, *120*, L15–L16. Bolzati, C.; Refosco, F.; Tisato, F.; Bandoli, G.; Dolmella, A. *Inorg. Chim. Acta* **1992**, *201*, 7–10. Vries, N. D.; Jones, A. G.; Davison, A. *Inorg. Chem.* **1989**, *28*, 3728–3734.

Table 4. Summary of Crystal Data for Complexes **1a**, **5a**, **6a**, **6b**, and **4b**

	1a	6a	5a	6b	7	4b
formula	$C_{31}H_{26}OPReS_3 \cdot 0.5C_7H_8$	$C_{25}H_{21}OPClReS_2 \cdot 1.5C_6H_6$	$C_{20}H_{19}OPClReS_2$	$C_{27}H_{26}OPReS_3$	$C_{25}H_{20}OPReS_3$	$C_{28}H_{28}PReS_3$
fw, g	774.0	771.32	592.09	679.83	649.76	677.85
cryst syst	monoclinic	monoclinic	monoclinic	triclinic	monoclinic	monoclinic
space group	*C*2/*c*	*P*2(1)/*c*	*C*2/*c*	$P\bar{1}$	*P*2(1)/*n*	*P*2(1)/*n*
a, Å	33.844(6)	10.247(2)	17.345(4)	9.272(3)	10.870(3)	8.2037(14)
b, Å	9.5051(16)	30.973(6)	10.982(2)	11.444(3)	18.284(5)	19.187(3)
c, Å	22.643(4)	10.280(2)	23.929(5)	12.909(4)	12.674(3)	17.022(3)
α, deg	90	90	90	82.415(5)	90	90
β, deg	121.374(3)	100.432(3)	110.753(3)	80.987(4)	110.978(5)	95.461(3)
γ, deg	90	90	90	76.334(5)	90	90
V, Å^3	6219.1(18)	2181.6(5)	4262.4(16)	1308.1(6)	2351.9(6)	2667.2(8)
Z	8	4	8	2	4	4
D(calcd), Mg/m^3	1.652	1.596	1.845	1.726	1.835	1.688
abs coeff, mm^{-1}	4.188	4.076	6.105	4.964	5.517	4.866
GOF	1.035	1.123	1.079	0.953	1.090	1.028
$R1$,[a] $wR2$[b] [$I > 2\sigma(I)$]	0.0299, 0.0692	0.0502, 0.1062	0.0447, 0.0960	0.0364, 0.0893	0.0405, 0.1092	0.0264, 0.0596

[a] $R1 = \sum||F_o| - |F_c||/\sum|F_o|$. [b] $wR2 = \{\sum[w(F_o^2 - F_c^2)^2]/\sum[w(F_o^2)^2]\}^{1/2}$.

provide a relative measure of the electrophilicity of the complexes.[21] The trend illustrates the influence of ligand variation on electron density at Re≡O. The methyl ligand is a much better σ donor, and phenoxide is both a good σ donor and a much stronger π donor,[22] as compared with PhS. The effect is to leave more electron density on Re, raising the LUMO energy and reducing the contribution of the 2p orbital of the oxygen atom to the LUMO. These factors are consistent with the observed lower electrophilic reactivity of those complexes. Replacement of the mtp ligand by an edt ligand makes complex **5b** more electron rich and thus decreases its reactivity compared to that of **1a**. This point needs to be emphasized. Reactivity is determined in the initial step, in which nucleophilic phosphine attacks the oxo group of [PhSReO(dt)(PPh_3)]. It is not sufficient to argue that the *ultimate* product from the edt complex, with a four-membered chelate ring, will be less stable than that from mtp or pdt, with five-membered rings. That argument may well apply to the subsequent steps, but not to the rate-controlling step. This is the reason for emphasizing the first step.

The issues surrounding the failure of [PhSReO(edt)PPh_3], **5b**, and [EtSReO(edt)PPh_3], **5c**, to react need to be addressed further. It is too facile simply to comment that the products, with four-membered chelate rings, would be too unstable. Single-electron reduction of [PhSReO(pdt)PPh_3], **3a**, is only marginally easier than that of **5b**. Further, the usage of single-electron E_{pc} values in describing atom transfer chemistry may not be on secure grounds, although others have made use of it.[21]

The best comparison can be made between **3a** and **5b** because they both contain alkanedithiolato ligands. It seems probable, therefore, that the initial PPh_3 attack leads to an intermediate that more resembles Re═O···PPh_3 than Re^{III}←OPPh_3. The edt complex cannot pass through the transition state, however, because of ring strain. Thus, PPh_3 is released and no net reaction occurs.

The values of $-E_{pc}$ for [XReO(mtp)(PPh_3)] (X = SPh, SEt, Cl, and *o*-$SC_6H_4P(Ph)_2$) fall into a small range, 0.84−1.04 V. Because **1a** and **6b** react with PPh_3 to promote C−S bond cleavage, it can expected that **6a** and **7** would undergo the same reaction, given that their similar E_{pc} values are slightly more anodic than those for **1a** and **6b**. This not the case. The difference in reactivity is most likely due to the different π-donating ability of ancillary ligands X. The chloro ligand is a poor π-donor and is expected to interact weakly with Re d−π orbitals. Chelation in **7** inhibits rotation about the Re−S bond, thus significantly weakening the S→Re π-donation because the thiolate−metal interaction depends on the Re−S−C(X) angle and the Re−S−C^{1-C2}(X) dihedral angle.[23] The Re−S bonds in **1a** and **6b** rotate, which enhances the interaction that induces C−S cleavage. It is the S→Re π-donation and the formation of stable five-membered rings that provide the driving force for C−S activation.

Conclusions

The preparation and thorough characterization of a series of oxorhenium(V) complexes that possess various types of ancillary ligands, chelate ligands, and dithiolates have allowed us to probe the influences of each of these variables on C−S activation. In particular, it has proved possible to focus on the nature of ligand→Re π-interactions. Spectroscopic, electrochemical, structural, and kinetic data reveal the critical role played by ligand→Re π-interactions in regioselective C−S bond cleavage reactions.

Experimental Section

All operations were carried out under an atmosphere of argon or nitrogen using standard Schlenk techniques unless other stated. Benzene, toluene, diethyl ether, THF, and hexane were distilled from sodium; dichloromethane was distilled from calcium hydride. Other reagents were used as received unless otherwise noted. Preparation of the dimers, {ReO(dt)(SPh)}$_2$, where H_2dt represents 2-(mercaptomethyl)thiophenol, 1,2-ethanedithiol, 1,3-propanedithiol, and 1,3-butanedithiol, has been reported elsewhere.[5] 2-(Diphenylphosphino)benzenethiol,[24] [Cl_3ReO-

(20) Meyer, T. J.; Huynh, M. H. V. *Inorg. Chem* **2003**, *42*, 8140−8160. Crevier, T. J.; Bennett, B. K.; Soper, J. D.; Bowman, J. A.; Dehestani, A.; Hrovat, D. A.; Lovell, S.; Kaminsky, W.; Mayer, J. M. *J. Am. Chem. Soc.* **2001**, *123*, 1059−1071.
(21) Dehestani, A.; Kaminsky, W.; Mayer, J. M. *Inorg. Chem* **2003**, *42*, 605−611. Bennett, B. K.; Crevier, T. J.; DuMez, D. D.; Matano, Y.; McNeil, W. S.; Mayer, J. M. *J. Organomet. Chem.* **1999**, *591*, 96−103.
(22) Chisholm, M. H.; Davidson, E. R.; Huffman, J. C.; Quinlan, K. B. *J. Am. Chem. Soc.* **2001**, *123*, 9652−9664.
(23) Davis, M. I.; Orville, A. M.; Neese, F.; Zaleski, J. M.; Lipscomb, J. D.; Solomon, E. I. *J. Am. Chem. Soc.* **2002**, *124*, 602−614. Fox, D. C.; Fiedler, A. T.; Halfen, H. L.; Brunold, T. C.; Halfen, J. A. *J. Am. Chem. Soc.* **2004**, *126*, 7627−7638. Solomon, E. I.; Szilagyi, R. K.; George, S. D.; Basumallick, L. *Chem. Rev.* **2004**, *104*, 419−458. Fiedler, A. T.; Halfen, H. L.; Halfen, J. A.; Brunold, T. C. *J. Am. Chem. Soc.* **2005**, *127*, 1675−1689.
(24) Block, E.; Ofori-Okai, G.; Zubieta, J. *J. Am. Chem. Soc.* **1989**, *111*, 2327−2329.

$(PPh_3)_2$],[25] and 2,4-pentanedithiol (H_2pdtMe_2)[26] were synthesized according literature procedures.

Infrared spectra were collected with a Bruker IFS66V FT-IR spectrometer as KBr pellets. NMR spectra were obtained on a Bruker DRX-400 at 298 K, with ^{1}H NMR chemical shifts referenced internally to the C_6D_6 solvent peak at δ 7.16 and the CD_2Cl_2 solvent peaks at δ 5.32; the ^{31}P NMR chemical shifts are referenced externally to 85% aqueous H_3PO_4. UV−visible spectra were recorded on benzene solutions at 298 K in quartz cuvettes using a Shimadzu UV-3101PC spectrophotometer with a temperature-controlled unit. Elemental analyses were performed at Iowa State University's Analysis Center with a Perkin-Elmer CHN/S analyzer, model 2400-II.

Cyclic voltammograms were measured with a BAS-100 potentiostat using a three-compartment cell with an $Ag/AgNO_3$ (0.1 mol L^{-1} in CH_3CN) reference electrode, a platinum-disk working electrode, and a platinum-wire auxiliary electrode. The electrolyte solution was 0.1 mol L^{-1} tetra-*n*-butylammonium tetrafluoroborate in CH_2Cl_2. The solution in the working compartment was kept anaerobic under an atmosphere of N_2. Potentials are reported relative to the SCE.

[PhSReO(mtp)(PPh$_3$)] (1a). A glass flask was charged with the dimer {PhSReO(mtp)}$_2$ (187 mg, 0.20 mmol), toluene (40 mL), and PPh_3 (105.7 mg, 0.40 mmol). The mixture was stirred at ambient temperature for 2 h, yielding a green solution which was then evaporated to dryness in vacuo. The residue was washed with diethyl ether to give pure **1a**, 230 mg, 80%. Dark green crystals were obtained from CH_2Cl_2−hexanes. NMR: ^{1}H (CD_2Cl_2), δ 7.79−7.73 (m, 6H), 7.56−7.54 (m, 2H), 7.50−7.46 (m, 9H), 7.39−7.36 (m, 2H), 7.29−7.22 (m, 3H), 7.18−7.14 (m, 2H), 4.95 (dd, J_1 = 12 Hz, J_2 = 1.6 Hz, 1H), 3.30 (d, J = 12 Hz, 1H); ^{31}P (CD_2Cl_2), δ 18.6. IR (KBr pellet): 946 cm^{-1} (s, $\nu_{Re\equiv O}$). UV−visible (C_6H_6): λ_{max}/nm (log ϵ), 580 (2.70), 427(3.46), 369 (3.64). Anal. Found (calcd) for $C_{31}H_{26}S_3PORe\cdot 0.5C_7H_8$: C, 53.39 (53.54); H, 3.62 (3.91); S, 11.66 (12.43); P, 3.41 (4.00).

[PhSReO(edt)(PPh$_3$)] (5b). Yield: 69%. NMR: ^{1}H (CD_2Cl_2), δ 7.80−7.75 (m, 6H), 7.51−7.48 (m, 9H), 7.47−7.45 (m, 2H), 7.34−7.31 (m, 2H), 7.22−7.19 (m, 1H), 3.79−3.68 (m, 2H), 2.62−2.51 (m, 2H); ^{31}P (CD_2Cl_2), δ 21.7. IR (KBr pellet): 949 cm^{-1} (s, $\nu_{Re\equiv O}$). UV−visible (C_6H_6): λ_{max}/nm (log ϵ), 620 (1.72), 531 (2.45), 411 (3.55), 327(sh) (3.62). Anal. Found (calcd) for $C_{26}H_{24}S_3PORe$: C, 46.40 (46.90); H, 3.47 (3.63); S, 13.98 (14.45).

[PhSReO(pdt)(PPh$_3$)] (3a). In an NMR tube, the dimer {PhSReO(pdt)}$_2$ (6.68 mg, 8.0 μmol) and PPh_3 (4.31 mg, 16 μmol) were mixed in CD_2Cl_2. After about 30 min, the solution color changed from brown to green. NMR: ^{1}H, δ 7.84−7.79 (m, 6H), 7.59−7.46 (m, 9H), 7.40−7.28 (m, 4H), 7.23−7.19 (m, 1H), 3.43−3.39 (m, 1H), 3.33−3.24 (m, 1H), 3.13−3.10 (m, 1H), 3.03−2.96 (m, 1H), 2.25−2.46 (m, 1H), 2.40−2.31 (m, 1H); ^{31}P, δ 17.7.

[ClReO(mtp)(PPh$_3$)] (6a). The reaction was conducted in air. 2-(Mercaptomethyl)thiophenol ($mtpH_2$, 187.6 mg, 1.2 mmol) in 20 mL of toluene was added dropwise to a yellow suspension of [Cl_3ReO(PPh$_3$)$_2$] (1.0 g, 1.2 mmol) in 280 mL of toluene, generating a clear green solution after several minutes. The reaction mixture was stirred at ambient temperature for 30 min and then filtered. The solvent was removed by rotary evaporation to afford a solid, which was washed with diethyl ether to give the pure green product (675 mg, 97%). NMR: ^{1}H (CD_2Cl_2), δ 7.70−7.65 (m, 6H), 7.58−7.43 (m, 9H), 7.34−7.31 (m, 3H), 7.23−7.19 (t, 1H), 5.14 (d, J = 11.6 Hz, 1H), 3.50 (d, J = 11.6 Hz, 1H); ^{31}P (CD_2Cl_2), δ 23.0. IR (KBr pellet): 975 cm^{-1} (s, $\nu_{Re\equiv O}$). UV−visible (C_6H_6): λ_{max}/nm (log ϵ), 649 (1.77), 437 (2.94), 362 (3.37). Anal. Found (calcd) for $C_{25}H_{21}S_3RePCl\cdot 0.5C_4H_{10}O$: C, 46.81 (46.91); H, 3.77 (3.79); S, 8.59 (9.27).

[X-*p*-C$_6$H$_4$SReO(mtp)(PPh$_3$)] (X = OMe, Me, F, Cl). A solution of **6a** (98 mg, 0.15 mmol) in 60 mL of benzene was transferred by cannula to a white suspension of $LiSC_6H_4$-*p*-X (from HSC_6H_4-*p*-X and BuLi) in a 1:1 mmol ratio. The resulting mixture was stirred for 2 h and then filtered. The solvent was evaporated to yield the solid products. Pure products were obtained after the solids were washed with diethyl ether.

X = OMe (1b). Yield: 66%. NMR: ^{1}H (CD_2Cl_2), δ 7.78−7.73 (m, 6H), 7.58−7.45 (m, 9H), 7.41−7.36 (m, 2H), 7.28−7.24 (m, 3H), 7.14−7.10 (m, 1H), 6.93−6.90 (m, 1H), 4.93 (dd, Hz, J_1 = 12 Hz, J_2 = 1.6, 1H), 3.38 (s, 3H), 3.29 (d, J_1 = 12 Hz, 1H); ^{31}P (CD_2Cl_2), δ 18.8. IR (KBr pellet): 947 cm^{-1} (s, $\nu_{Re\equiv O}$). UV−visible (C_6H_6): λ_{max}/nm (log ϵ), 584 (2.72), 428 (3.43), 370 (3.59). Anal. Found (calcd) for $C_{32}H_{28}S_3PO_2Re$: C, 51.16 (50.71); H, 4.32 (3.72); S, 12.07 (12.69).

X = Me (1c). Yield: 65%. NMR: ^{1}H (CD_2Cl_2), δ 7.78−7.73 (m, 6H), 7.57−7.46 (m, 9H), 7.37−7.35 (m, 2H), 7.27−7.24 (m, 3H), 7.21−7.19 (m, 2H), 7.13−7.10 (m, 1H), 4.94 (dd, J_1 = 12 Hz, J_2 = 1.6 Hz, 1H), 3.29 (d, J_1 = 12 Hz, 1H), 2.43 (s, 3H). ^{31}P NMR (CD_2Cl_2), δ 18.6. IR (KBr pellet): 950 cm^{-1} (s, $\nu_{Re\equiv O}$). UV−visible (C_6H_6): λ_{max}/nm (log ϵ), 581 (2.58), 428 (3.37), 370 (3.52). Anal. Found (calcd) for $C_{32}H_{28}S_3PORe$: C, 51.67 (51.80); H, 4.26 (3.80); S, 12.36 (12.97).

X = F (1d). Yield: 68%. NMR: ^{1}H (CD_2Cl_2) δ 7.77−7.73 (m, 6H), 7.57−7.45 (m, 9H), 7.37−7.35 (m, 2H), 7.27−7.25 (m, 3H), 7.15−7.10 (m, 1H), 7.09−7.06 (m, 2H), 4.96 (dd, J_1 = 12 Hz, J_2 = 1.6 Hz, 1H), 3.30 (d, J_1 = 12 Hz, 1H); ^{31}P NMR (CD_2Cl_2), δ 18.8. IR (KBr pellet): 953 cm^{-1} (s, $\nu_{Re\equiv O}$). UV−visible (C_6H_6): λ_{max}/nm (log ϵ), 578 (2.75), 430 (3.43), 370 (3.63). Anal. Found (calcd) for $C_{31}H_{25}S_3POFRe$: C, 50.58 (49.92); H, 4.02 (3.38); S, 11.70 (12.90).

X = Cl (1e). Yield: 51%. NMR: ^{1}H (CD_2Cl_2), δ 7.77−7.72 (m, 6H), 7.57−7.46 (m, 9H), 7.45−7.43 (m, 2H), 7.36−7.33 (m, 2H), 7.28−7.25 (m, 3H), 7.15−7.12 (m, 1H), 4.96 (dd, J_1 = 12 Hz, J_2 = 1.6 Hz, 1H), 3.30 (d, J_1 = 12 Hz, 1H); ^{31}P (CD_2Cl_2), δ 18.8. IR (KBr pellet): 955 cm^{-1} (s, $\nu_{Re\equiv O}$). UV−visible (C_6H_6): λ_{max}/nm (log ϵ), 579 (2.65), 428 (3.39), 370 (3.58). Anal. Found (calcd) for $C_{31}H_{25}S_3POClRe$: C, 48.97 (48.84); H, 3.91 (3.31); S, 11.85 (12.62).

[C$_2$H$_5$SReO(mtp)(PPh$_3$)] (6b). This compound was prepared in 48% yield by the reaction of **6a** and 1.0 equiv of $LiSC_2H_5$ (obtained as a green solid from C_2H_5SH and BuLi) in a procedure analogous to the method for [X-*p*-C_6H_4SReO(mtp)(PPh_3)]. NMR: ^{1}H (CD_2Cl_2), δ 7.74−7.69 (m, 6H), 7.54−7.44 (m, 9H), 7.42−7.41 (m, 1H), 7.37−7.33 (m, 1H), 7.30−7.28 (m, 1H), 7.19−7.16 (m, 1H), 4.92 (dd, J_2 = 12 Hz, J_1 = 1.6 Hz, 1H), 3.89−3.82 (m, 1H), 3.73−3.64 (m, 1H), 3.35 (d, J_1 = 12 Hz, 1H), 1.45 (t, J = 7.2 Hz, 3H); ^{31}P (CD_2Cl_2), δ 18.5. IR (KBr pellet): 950 cm^{-1} (s, $\nu_{Re\equiv O}$). UV−visible (C_6H_6): λ_{max}/nm (log ϵ), 595 (2.57), 426(sh) (3.40), 392 (3.48), 350 (3.51). Anal. Found (calcd) for $C_{27}H_{26}S_3PORe$: C, 48.64 (47.70); H, 4.30 (3.85); S, 13.60 (14.15).

[*o*-Ph$_2$PC$_6$H$_4$SReO(mtp)] (7). This compound was prepared in 82% yield with Li[*o*-$SC_6H_4P(Ph)_2$] in a procedure analogous to the method for [C_2H_5SReO(mtp)(PPh_3)]. NMR: ^{1}H (CD_2Cl_2), δ 8.01−7.99 (m, 1H), 7.89−7.84 (m, 2H), 7.58−7.47 (m, 7H), 7.43−7.38 (m, 2H), 7.34−7.29 (m, 2H), 7.25−7.17 (m, 4H), 5.07 (dd, J_1 = 1.2 Hz, J_2 = 12 Hz, 1H), 3.25 (d, J_1 = 12 Hz, 1H); ^{31}P (CD_2Cl_2), δ 55.9. IR (KBr pellet): 966 cm^{-1} (s, $\nu_{Re\equiv O}$). UV−visible (C_6H_6): λ_{max}/nm (log ϵ), 565 (2.54), 448 (sh) (3.04), 380 (2.53), 344 (3.92). Anal. Found (calcd) for $C_{25}H_{20}S_3PORe\cdot 0.5C_4H_{10}O$: C, 48.18 (47.21); H, 3.57 (3.69); S, 13.75 (14.00).

[PhOReO(mtp)(PPh$_3$)] (6c). A solution of **6a** (222 mg, 0.34 mmol) in THF (60 mL) was dropwise added to a solution of LiOPh (0.34 mmol) (from PhOH and BuLi), the resulting solution was stirred overnight, and then the solvents were removed in vacuo. The residue was dissolved in benzene (50 mL) and then filtered. The filtration was reduced to dryness and the obtained solid washed with diethyl ether to give the product (61 mg, 25%). NMR: ^{1}H (CD_2Cl_2), δ 7.56−7.48 (m, 8H), 7.40−7.33 (m, 10H), 7.25−7.23 (m, 2H), 7.12−7.08 (m, 2H), 7.06−7.02 (m, 2H), 4.77 (d, J = 12 Hz, 1H), 3.37 (d, J = 12 Hz, 1H); ^{31}P (CD_2Cl_2), δ 32.5. IR (KBr pellet): 949 cm^{-1} (s, $\nu_{Re\equiv O}$). UV−visible (C_6H_6): λ_{max}/nm (log ϵ), 557 (2.74), 458 (3.07), 352 (3.62). Analytically pure solids could not be isolated by column chromatography due to decomposition.

(25) Chatt, J.; Rowe, A. *J. Chem. Soc.* **1962**, 4019−4033.
(26) Overberger, C. G.; Ferraro, J. J.; Orttung, F. W. *J. Org. Chem* **1961**, *26*, 3458−3460.

[ClReO(edt)(PPh$_3$)] (5a). The procedure was as described for **6a**: 1.0 g of [Cl$_3$ReO(PPh$_3$)$_2$] (1.2 mmol) and 101 μL of 1,2-ethanedithiol (H$_2$edt, 1.2 mmol) gave, after being stirred for 30 min and worked up similarly, 632 mg of a green solid (89%). NMR: ^{1}H (CD$_2$Cl$_2$), δ 7.71−7.66 (m, 6H), 7.55−7.46 (m, 9H), 3.87−3.79 (m, 2H), 3.03−2.97 (m, 1H), 2.78−2.69 (m, 1H); ^{31}P (CD$_2$Cl$_2$), δ 27.3. IR (KBr pellet): 978 cm^{-1} (s, $\nu_{Re\equiv O}$). UV−visible (C$_6$H$_6$): λ_{max}/nm (log ϵ), 581 (1.97), 415 (3.42), 328 (3.48). Anal. Found (calcd) for C$_{20}$H$_{19}$S$_2$POClRe: C, 40.10 (40.57); H, 3.33 (3.23); S, 10.02 (10.83).

[C$_2$H$_5$SReO(edt)(PPh$_3$)] (5c). A similar procedure was employed to obtain this product in 66% yield as described for [C$_2$H$_5$SReO(mtp)(PPh$_3$)]. NMR: ^{1}H (CD$_2$Cl$_2$), δ 7.75−7.71 (m, 6H), 7.54−7.44 (m, 9H), 3.94−3.92 (m, 1H), 3.82−3.73 (m, 1H), 3.65 (q, J = 7.6 Hz, 2H), 2.64−2.50 (m, 2H), 1.38 (t, J = 7.6 Hz, 3H); ^{31}P (CD$_2$Cl$_2$), δ 20.8. IR (KBr pellet): 952 cm^{-1} (s, $\nu_{Re\equiv O}$). UV−visible (C$_6$H$_6$): λ_{max}/nm (log ϵ), 642 (1.61), 524 (2.44), 396 (3.60). Anal. Found (calcd) for C$_{22}$H$_{24}$S$_3$PORe·0.5H$_2$O: C, 41.75 (42.15); H, 4.23 (4.02); S, 15.44 (15.35).

[ReS(SC$_6$H$_4$CH$_2$)(SC$_6$H$_4$-*p*-X))(PPh$_3$)] (X = OMe, Me, F, Cl) (2b−e). These complexes were all generated in procedures analogous to that described for **2a**. We had no attempt to isolate the products to be fully characterized in pure form. The^{1}H and ^{31}P NMR spectra of the products are quite similar to those observed for **2a**.[2]

[ReS(SC$_6$H$_4$CH$_2$)(SC$_2$H$_5$)(PPh$_3$)] (8). A glass flask was charged with [C$_2$H$_5$SReO(mtp)(PPh$_3$)] (147 mg, 0.22 mmol), benzene (100 mL), and PPh$_3$ (284 mg, 1.08 mmol). The mixture was stirred at ambient temperature for 5 days as the brown solution developed gradually. The solvent was reduced to dryness, and the residue was dissolved in a minimal volume of diethyl ether, loaded on a silica gel column, and eluted with hexanes−ether. The red-brown band was collected, and upon removal of the solvents a brown solid was obtained (20 mg, 14%). NMR: ^{1}H (CD$_2$Cl$_2$), δ 7.79 (br, 6H), 7.61 (br, 2H), 7.52−7.45 (m, 9H), 7.12 (br, 2H), 6.67 (d, J = 16.4 Hz, 1H), 4.09 (dd, J_1 = 16.4 Hz, J_2 = 9.6 Hz, 1H), 3.56 (q, J = 6.8 Hz, 2H), 1.55 (t, J = 6.8 Hz, 3H); ^{31}P NMR (CD$_2$Cl$_2$), δ 35.1. IR (KBr pellet): 521 cm^{-1} (s, $\nu_{Re\equiv S}$). UV−visible (C$_6$H$_6$): λ_{max}/nm (log ϵ), 611 (1.68), 488 (3.16), 371 (4.04), 320 (3.93). Anal. Found (calcd) for C$_{27}$H$_{26}$S$_3$PRe: C, 48.21 (48.85); H, 4.60 (3.95); S, 13.62 (14.49).

[PhSReS(−SCHMeCH$_2$CH$_2$−)(PPh$_3$)] (4b) and [PhSReS(−SCH$_2$CH$_2$CHMe−)(PPh$_3$)] (4c). A mixture of {PhSReO(pdtMe)}$_2$ (241.7 mg, 0.28 mmol) and PPh$_3$ (347 mg, 1.32 mmol) was dissolved in toluene (70 mL). The color of the solution rapidly changed from brown to yellowish as the reaction mixture was stirred at ambient temperature for 5 days and then filtered. The filtrate was evaporated to give a residue, which was dissolved in a minimal volume of diethyl ether. Column chromatography afforded a yellowish band, which was collected by eluting with ether−hexane; following that, the solvents were removed to give a solid. The pure product was obtained by washing with cool ether (yield 266 mg, 70%). IR (KBr pellet): 524 cm^{-1} (s, $\nu_{Re\equiv S}$). UV−visible (C$_6$H$_6$): λ_{max}/nm (log ϵ), 594 (1.59), 458 (2.86), 386 (sh, 3.48), 337 (sh, 3.97). 324 (3.99). Anal. Found (calcd) for C$_{28}$H$_{28}$S$_3$PRe: C, 49.63 (49.61); H, 4.60 (4.16); S, 14.08 (14.19).

4b. NMR: ^{1}H (C$_6$D$_6$), δ 8.05 (br, 6H), 7.89−7.85 (m, 2H), 7.18−7.14 (m, 2H), 7.06−6.96 (m, 10H), 5.68 (br, d, J = 14 Hz, 1H$_a$), 3.42−3.31 (m, 1H$_b$), 3.22−3.17 (m, 1H$_c$), 2.79−2.71(m, 1H$_e$), 1.79−1.68 (m, 1H$_d$), 1.55 (d, J = 6.8 Hz, CH_3); ^{13}C (C$_6$D$_6$), δ 151.63, 151.52, 135.70, 135.60, 135.01, 134.49, 133.73, 133.69, 131.22, 131.20, 129.06, 128.94, 128.84, 127.32, 59.43 (d, *C*H$_e$), 58.72 (d, *C*H$_a$H$_b$), 50.38 (*C*H$_c$H$_d$), 21.78 (*C*H$_3$); ^{31}P (C$_6$D$_6$), δ 31.8.

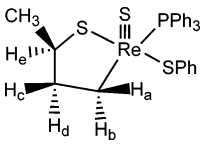

4c. NMR: ^{1}H (C$_6$D$_6$), δ 8.05 (br, 6H), 7.89−7.85 (m, 2H), 7.18−7.14 (m, 2H), 7.06−6.96 (m, 10H), 5.62 (br d, 1H$_a$), 3.87−3.77 (m, 1H$_b$), 3.74−3.67 (m, 1H$_e$), 2.79−2.71 (m, 1H$_c$), 2.31−2.20 (m, 1H$_d$), 0.96 (d, J = 6.8 Hz, CH_3); ^{13}C, δ 151.52, 151.39, 135.70, 135.60, 134.78, 134.27, 133.73, 133.69, 131.22, 131.20, 129.10, 128.89, 128.78, 127.27, 59.63 (d, *C*H$_e$), 57.56 (d, *C*H$_a$H$_b$), 48.50 (*C*H$_c$H$_d$), 20.60 (*C*H$_3$); ^{31}P (C$_6$D$_6$), δ 32.3.

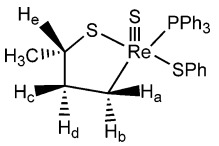

{PhS(ReO)(pdtMe$_2$)}$_2$. 2,4-Pentanedithiol (103.2 mg, 0.76 mmol) was added by syringe to a suspension of {(ReO)(SPh)$_3$}$_2$ (401 mg, 0.0.38 mmol) in toluene (90 mL), and the mixture was stirred overnight under N$_2$ and then filtered. The red-brown filtrate was evaporated to dryness and dissolved in CH$_2$Cl$_2$ (∼2 mL), which was loaded on silica gel. The first brown band was collected. Upon removal of the solvent, the obtained solid was washed with ether and vacuum-dried. Yield: 70 mg, 20%. ^{1}H NMR (complicated owing to diastereomers) (CD$_2$Cl$_2$): δ 7.48−7.33 (m, 8H), 7.29−7.24 (m, 2H), 4.40−4.38 (m, 1H), 4.15−4.07 (m, 1H), 3.59−3.46 (m, 1H), 3.33−3.26 (m, 1H), 3.13−3.08 (m, 1H), 2.99−2.83 (m, 1H), 1.81−1.77 (m, 6H), 1.42−1.34 (m, 3H), 1.22−1.20, 1.21 (dd, J = 6.8 Hz, 3H). Anal. Found (calcd) for C$_{22}$H$_{30}$O$_2$S$_6$Re$_2$: C, 29.77 (29.65); H, 3.58 (3.39); S, 20.83 (21.59).

[ReS(−SCHMeCH$_2$CHMe−)(SPh)(PPh$_3$)] (4d). Reaction of {PhS(ReO)(pdtMe$_2$)}$_2$ with excess PPh$_3$ in C$_6$D$_6$ (∼0.8 mL) was monitored by ^{1}H and ^{31}P NMR spectroscopy at 25 °C. NMR: ^{1}H (C$_6$D$_6$) (aryl region, overlapping with PPh$_3$ and OPPh$_3$), δ 6.11−6.05 (m, 1H), 3.97−3.93 (m, 1H), 2.61−2.54 (m, 1H), 2.40−2.33 (m, 1H), 2.41 (d, J = 6.8 Hz, 3H), 1.21 (d, J = 6.8 Hz, 3H); ^{31}P (C$_6$D$_6$), δ 24.9.

Kinetics Measurements. Reactions of the monomers with the phosphines were monitored by UV−visible spectra with an Agilent 8453 spectrophotometer with a pseudo-first-order excess of phosphine in benzene solution at 25.0 ± 0.2 °C. Initial monomeric Re(V) complex concentrations were [Re(V)]$_0$ = 0.08−0.23 mmol L^{-1} in systems containing 10−8000 equiv of phosphine. As the reactions proceeded, the solution color changed from green to red-brown in the mtp series, or from green to yellowish in the pdt series. Data analysis is described in the Results.

X-ray Structure Determinations. The structures of the complexes in Table 4 were determined by X-ray crystallography. Selected crystals were mounted on a Siemens (Bruker) SMART 1000 CCD diffractometer equipped with a low-temperature apparatus. Mo Kα radiation (λ = 0.71073 Å) was used for data collection. Data were collected using the full sphere routine with 0.3° scans in ω with an exposure time 10−30 s/frame. Final cell parameters were retrieved by using SMART software and refined by using SAINT software, which corrects for Lorentz polarization and decay; absorption corrections were applied with SADABS.[27] The space groups for all the complexes were assigned unambiguously by analysis of symmetry and systematic absences determined by the program XPREP.

The structures were solved by direct or Patterson methods. The positions of the heavy atoms were found directly by both methods; the remaining atoms were located in an alternating series of least-squares cycles and difference Fourier maps. All non-hydrogen atoms were refined in full-matrix anisotropic approximation; all hydrogen atoms were placed in the structure factor calculation at idealized positions and were allowed to ride on the neighboring atoms with relative isotropic displacement coefficients.

(27) All software and sources of the scattering factors are contained in the SHELXTL (version 5.1) program library (Sheldrick, G. M., Bruker Analytical X-ray Systems, Madison, WI).

Acknowledgment. This research was supported by the U.S. Department of Energy, Office of Basic Energy Science, Division of Chemical Sciences, under Contract W-7405-Eng-82 with Iowa State University. We thank Adam J. Bergren for assistance with the electrochemistry and Steven Veysey for the elemental analyses.

Supporting Information Available: 2D COSY spectrum and ^{1}H NMR spectra of the isomers **4b** and **4c** in C_6D_6 at 25 °C (Figures S1 and S2); linear correlations of k_{obs} vs triarylphosphines concentration (Figures S3−S7); plot of log k_2 vs numbers of the methyl groups on the pdt framework (Figure S8); cyclic voltammograms of the complexes with $Re^{V}O$ core (Figures S9−S15) (PDF); complete crystallographic data for **1a**, **5a**, **6a**, **6b**, **7**, and **4b** (CIF). This material is available free of charge via the Internet at http://pubs.acs.org.

JA0519334